

Research Paper

Optimization of Metallic Catalytic Converters to Reduce CO Emissions and Increase Engine Power

Warju¹✉, Sudirman Rizki Ariyanto¹, Muhammad Yandi Pratama², Kusuma Refa Haratama³

¹Department of Automotive Engineering Technology, Faculty of Vocational Studies, Universitas Negeri Surabaya, 60231, Indonesia

²Department of Mechanical Engineering and Industries, Faculty of Engineering, Universitas Negeri Malang, 65145, Indonesia

³Department of Transportation, Faculty of Vocational Studies, Universitas Negeri Surabaya, 60231, Indonesia

✉ warju@unesa.ac.id

🌐 <https://doi.org/10.31603/ae.11567>

Published by Automotive Laboratory of Universitas Muhammadiyah Magelang

Abstract

Article Info

Submitted:

19/06/2024

Revised:

30/07/2024

Accepted:

05/08/2024

Online first:

18/09/2024

Metallic catalytic converter (MCC) is one of the technologies widely applied to motorcycle exhausts which aims to improve exhaust emission to be more environmentally friendly. However, even though many studies have been conducted, optimal design has not been achieved compared to other designs. Through this research, the Taguchi method is proposed as an alternative method to find the optimum parameters of MCC. The Taguchi method was chosen because of its ability to find a robust combination of parameters. There are four MCC parameters used as inputs while each parameter consists of three levels, thus the design used is the L18 Orthogonal Array (OA) which each combination is tested on three types of motorcycles, namely Moped, Automatic, and Sports. The signal-to-noise ratio (S/N) was adopted as one of the quality indicators of each combination. The optimization results showed that the best MCC design to reduce CO emissions is STD PGM. However, the optimum CO design can be used as an alternative because the difference in the S/N ratio is only -0.372. Meanwhile, the optimum CO design has another advantage over the STD PGM, namely the S/N value of the power ratio which tends to be higher with a difference of 5.037 compared to the STD PGM. Then, the best MCC design capable of increasing power is the optimum power design. The optimum power design has a superior S/N ratio with a difference of 5.404. In terms of emission, the optimum power design tends to be lower by a difference of -1.875 compared to the STD PGM.

Keywords: Metallic catalytic converter, Motorcycle; Taguchi method; CO emission; Engine power

1. Introduction

Addressing the impact of climate change is one of the contributions to achieving Goal 13 of sustainable development (SDGs) set by the UN in 2015 [1]–[4]. The proposed program is directed at strategic efforts to minimize the impact of air pollution, especially emissions from motor vehicles. Therefore, metallic catalytic converters (MCCs) installed in vehicle exhaust pipes are one approach to reducing emissions. The application

of MCCs is considered appropriate, considering that 65% to 85% of total emissions that spread into the environment cause health problems [5]. Automotive manufacturers prefer platinum group metals (PGM) or precious metals such as Platinum (Pt), Palladium (Pd), and Rhodium (Rh) as the base material for catalytic converters because of their effectiveness in reducing exhaust emissions [6]. However, precious metals are expensive and are designed to be installed on exhaust pipes [7].



This work is licensed under a Creative Commons Attribution-NonCommercial 4.0 International License.

Therefore, many researchers are exploring transition metals as catalytic converter materials [8]. Choudhury & Deo [9] claimed that the use of copper plate catalytic converters can reduce 55.44% HC, 62.96% CO, and 40.41% NO_x at full load conditions. Rathore, Thakur, & Deepak [10] conducted a study on copper catalytic converters coated with nanoparticles. The results showed that CO was reduced from 1.25% vol to 0.8% vol, HC from 962 ppm to 862 ppm. In addition, NO_x and CO₂ were also reported to be reduced consistently. The results of this study are in line with the research of Shoffan, Sumarli, & Nauri [11] which revealed that copper-based catalytic converters with a round tube design were proven to be able to reduce CO by 16.67%, and HC by 32.54%.

However, from the literature studied, the optimal design of MCC with transition metals has not been widely revealed. Therefore, this study was conducted to find a motorcycle exhaust design using MCC made of transition metals that is able to approach or even exceed the capabilities of MCC made of PGM, both in reducing exhaust emissions and increasing output power. The Taguchi method was chosen because of its reliability in design optimization [12]–[14].

2. Methods

2.1. Variables

In our present study, the variables set include (1) material type, (2) curve height, (3) cylinder diameter, and (4) MCC cylinder length. The outputs measured in each MCC design are CO content in exhaust gas and engine power. In this

case, CO is chosen because it has more serious health impacts than HC. Although HC is also a hazardous exhaust gas, exposure to CO can cause poisoning, even at low levels it can cause headaches and nausea. Meanwhile, the selection of power as the output is based on the need to evaluate the overall engine performance. In this case, torque only measures the engine's torque, which does not always directly reflect the overall engine efficiency or performance. The MCC design is presented in Figure 1 and the design variables are presented in Table 1.

The selection of MCC design variable parameters refers to our previous research [14]. In this study, the selection of levels for each variable is carried out by considering the availability of materials and space available on the exhaust to ensure that the MCC can be installed properly. The signal-to-noise ratio of the Taguchi method is used as a measure of design quality [15]. Furthermore, the measure of exhaust design quality can be assessed based on the average value and standard deviation considered simultaneously for each design [16]. Mtl, Ch, Cd, and Cl are the MCC design variables as shown in Table 1, while M and rpm are the type of motorcycle and engine speed. The type of motorcycle and engine speed are considered as uncertain magnitudes/noise factors. In this context, Liu et al. [17] argue that the selected process is considered ideal, although there are always factors that cause uncertainty in the process. In this research, three types of motorcycles (Moped, Automatic, and Sport) were tested with the L18 fractional orthogonal array experimental design.

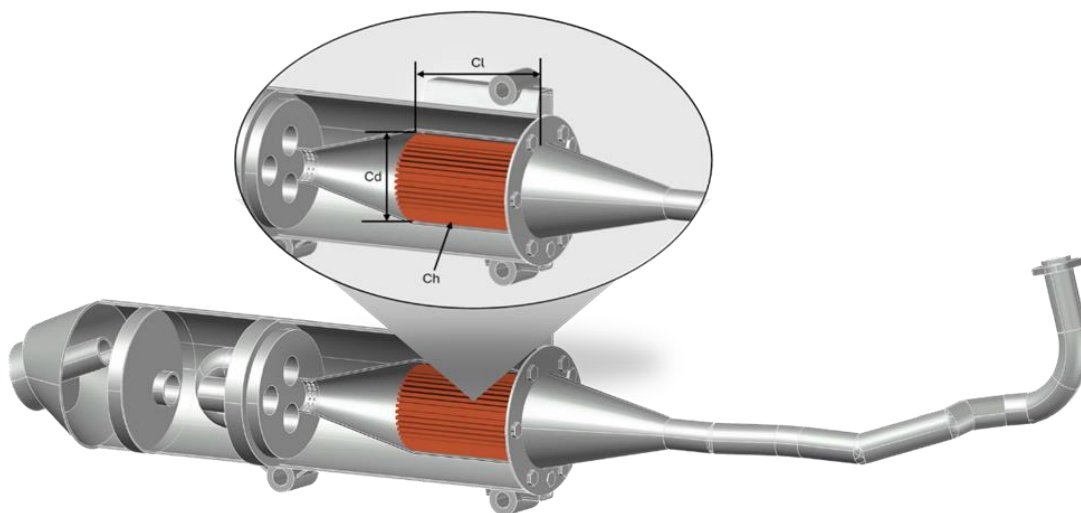


Figure 1. Visualization of MCC construction

Table 1. MCC design variables

| Control Factors | | L1 | L2 | L3 |
|-----------------|-----------------------|----|------|------|
| Mtl | Materials | Cu | CuZn | CuCr |
| Ch | Curve height, mm | 2 | 3 | 4 |
| Cd | Cylinder diameter, mm | 35 | 41 | 54 |
| Cl | Cylinder length, mm | 60 | 80 | 100 |

2.2. Optimization Strategy

The optimization strategy in this MCC design uses robust parameter design with the Taguchi method to identify the optimum design. The Taguchi method was chosen because it is known to be effective in optimizing the design process by considering minimal variation. The Taguchi method offers the advantage of reducing the number of trials required to achieve the optimum design, thus saving time and cost. In addition, this method excels in finding performance parameters that are robust to performance fluctuations due to uncertain conditions. The optimization strategy flow is shown in [Figure 2](#).

2.3. Research Equipment and Instruments

The details of the research equipment and instruments are presented in [Table 2](#). Testing was conducted on three types of motorcycles, namely Sports, Automatic, and Mopeds, namely Yamaha

Vixion Lightning, Honda Vario LED, and Honda Supra Fit. Testing was carried out under the same conditions, namely from 1000 to 9000 rpm. The selection of these three types of motorcycles is important because each type has its characteristics, while the ideal MCC design must be able to accommodate various types of motorcycles. By using the results of the CO study and the average power of the three test samples, the effect plot for CO and power can provide a comprehensive understanding of the effectiveness of MCC in reducing CO and maintaining engine performance on various types of motorcycles. To obtain valid and reliable research data, a testing method based on national and international standards was carried out, including SNI 09-7118.3-2005 [18] and Engine Power Test Code-Spark Ignition and Compression Ignition-Net Power Rating [19].

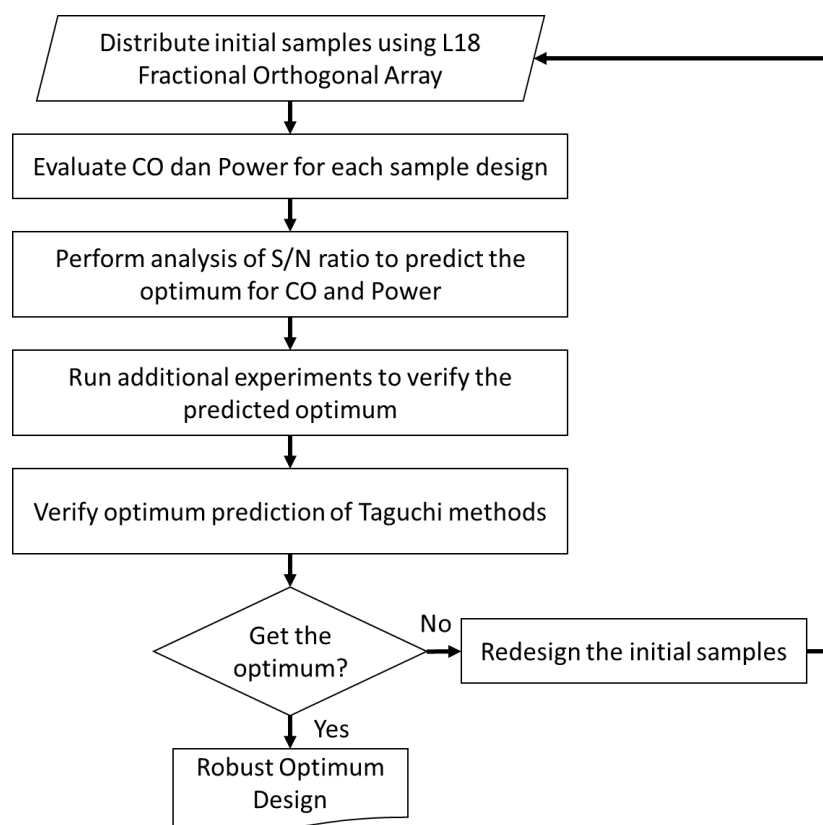
**Figure 2.** Robust flow diagram of MCC design parameters

Table 2. Specification research equipment and instruments

| Specification | Chassis Dynamometer | Exhaust Gas Analyzer | Blower |
|---------------|----------------------|----------------------|---------------------|
| Brand | Rextor Pro-Dyno | Heshbon HG-520 | Krisbow DIA 18 Inch |
| Voltage | 220V | 220V | 220V |
| Weight | 350 kg | 10 kg | 15 kg |
| Dimensions | 1500 x 1000 x 500 mm | 285 x 410 x 155 mm | 630 x 590 x 950 mm |

3. Results and Discussion

3.1. Result

A total of 18 MCC designs were tested for exhaust emissions and engine performance. The results of CO emissions and engine performance tests are shown in Table 3. Based on the test results, it can be stated that the overall MCC design can reduce CO emissions. This finding is in line with previous research conducted by Arvikar [20] which also showed that MCC is effective in reducing exhaust emissions. However, of the 18 designs, the largest reduction was in experimental design 16, namely for Moped by 30%, Automatic by 44%, and Sport by 21%. Experimental design 16 involved CuCr material with a curve height of 2 mm, a diameter of 54 mm, and a length of 80 mm. These results are in line with the results of research conducted by our previous study [21] which showed good performance of CuCr material in reducing CO emissions. MCC technology has also been shown to increase the power generated by Moped, Automatic, and Sport motorcycles. The best power increase was in experimental design 18 which is in line with the

research of Ariyanto et al. [14]. Experimental design 18 involved CuCr material, curve height of 4 mm, diameter of 41 mm, and length of 60 mm.

3.2. Optimization

The results of the CO and power tests from the L18 design that have been obtained are then used to determine the average value and standard deviation of each experimental result. The Taguchi method works by minimizing the standard deviation to reduce the noise produced [22]. After the average value and standard deviation are obtained, the calculation of the S/N ratio value is continued. The smaller the S/N ratio value to CO, the better, and the larger the S/N ratio value to power, the better [23]. This means that the smaller the CO value obtained, the better, while the larger the power value, the better [24], as formulated in Equation (2).

$$\text{Min. (CO)} = f(\text{Mtl, Ch, Cd, Cl; M, rpm}) \quad (1)$$

$$\text{Max. (Power)} = f(\text{Mtl, Ch, Cd, Cl; M, rpm}) \quad (2)$$

Table 3. CO emission and power test results

| Exp | Parameters | | | | CO (%) | | | Power (hp) | | |
|-----|------------|-------|----------|--------|--------|-----------|-------|------------|-----------|-------|
| | Material | Curve | Diameter | Length | Moped | Automatic | Sport | Moped | Automatic | Sport |
| E1 | Cu | 2 | 35 | 60 | 6.39 | 12.14 | 10.76 | 3.92 | 7.23 | 9.84 |
| E2 | Cu | 3 | 41 | 80 | 5.90 | 11.54 | 10.18 | 4.14 | 7.16 | 9.96 |
| E3 | Cu | 4 | 54 | 100 | 5.47 | 11.05 | 9.21 | 4.19 | 7.21 | 8.44 |
| E4 | CuZn | 2 | 35 | 80 | 6.47 | 12.26 | 10.89 | 3.78 | 6.57 | 6.91 |
| E5 | CuZn | 3 | 41 | 100 | 5.92 | 11.67 | 10.24 | 3.78 | 7.19 | 9.84 |
| E6 | CuZn | 4 | 54 | 60 | 6.59 | 12.77 | 11.07 | 4.33 | 6.86 | 10.04 |
| E7 | CuCr | 2 | 41 | 60 | 5.71 | 11.24 | 9.37 | 4.16 | 7.17 | 9.93 |
| E8 | CuCr | 3 | 54 | 80 | 5.36 | 10.86 | 9.17 | 4.15 | 7.19 | 10.00 |
| E9 | CuCr | 4 | 35 | 100 | 5.85 | 11.37 | 9.99 | 3.61 | 7.21 | 9.94 |
| E10 | Cu | 2 | 54 | 100 | 5.29 | 10.75 | 9.02 | 4.13 | 7.17 | 9.92 |
| E11 | Cu | 3 | 35 | 60 | 6.64 | 12.91 | 11.17 | 4.20 | 7.16 | 9.94 |
| E12 | Cu | 4 | 41 | 80 | 6.34 | 12.03 | 10.65 | 4.16 | 7.16 | 9.81 |
| E13 | CuZn | 2 | 41 | 100 | 5.75 | 11.25 | 9.57 | 4.29 | 7.16 | 8.38 |
| E14 | CuZn | 3 | 54 | 60 | 6.53 | 12.55 | 10.96 | 4.15 | 7.16 | 9.90 |
| E15 | CuZn | 4 | 35 | 80 | 6.77 | 12.97 | 11.32 | 4.06 | 7.14 | 9.84 |
| E16 | CuCr | 2 | 54 | 80 | 5.29 | 10.39 | 8.96 | 4.17 | 7.11 | 10.09 |
| E17 | CuCr | 3 | 35 | 100 | 5.6 | 11.18 | 9.31 | 4.12 | 6.94 | 9.97 |
| E18 | CuCr | 4 | 41 | 60 | 6.08 | 11.85 | 10.56 | 4.71 | 7.19 | 10.34 |

The obtained S/N ratio value is then used as a benchmark in determining the level of excellence of an experimental design based on the parameter settings that have been used. In more detail, the results of the calculation of the mean, standard deviation, and S/N ratio are shown in [Table 4](#).

From the data in [Table 4](#), it is known that the best MCC design based on the calculation of the S/N ratio was found in experiment 16, for the best CO emission, and experiment 18, for the best power. Experiment 16 resulted in an average value of CO emission from three vehicles of 2.74, standard deviation of 0.88, with an S/N ratio of -9,172. Meanwhile, experiment 18 resulted in the average power value of the three vehicles of 7.42, a standard deviation of 2.82, with an S/N ratio of 15,836. These findings are consistent with the research by Yu et al. [25], which stated that the S/N ratio is a reliable indicator for determining the best quality design in the optimization process. The two designs are the best designs based on the results of data processing. Furthermore, to ensure whether the two designs are the best for CO emission and power, further analysis is carried out. The analysis used was the effect analysis of the S/N ratio plot. S/N ratio plot effect analysis was used to describe a factor to an output, in this study the effect plot was used to represent each variation of the MCC parameter from three levels with four controlled parameters. This approach

has been successfully applied in other research studies [26]–[29] to find optimal designs in various fields.

In general, plot effects are depicted in the form of a line. When the line has a horizontal tendency, it can be interpreted that the output for each parameter does not change [30]. On the other hand, if the line has a skewed tendency in one of the outputs, then there is a significant change in certain parameters [22]. In more detail, the results of the plot effect analysis in this study are shown in [Figure 3](#) and [Figure 4](#).

Based on [Figure 3](#), the CO emission produced by the three types of vehicles can be reduced optimally if a combination of MCC Mtl 3, Ch 1, Cd 3, and Cl 3 is used. This means the robust parameter design method predicts that CO emission can be reduced optimally when using a combination of MCC which consists of CuCr material, curve height of 2 mm, cylinder diameter of 54 mm, and cylinder length of 100 mm. Then [Figure 4](#) shows that the power produced by the three types of vehicles can be increased optimally when using a combination of MCC Mtl 3, Ch 3, Cd 2, and Cl 1. This means the robust parameter design method predicts that power can be increased optimally when using a combination of MCC that consists of CuCr material, the indentation height is 4 mm, the cylinder diameter is 41 mm, and the cylinder length is 60 mm.

Table 4. CO and power data processing results

| Exp | CO | | | Power | | | Mean | | STDEV | | SNR | |
|-----|-------|-------|-------|-------|-------|-------|------|-------|-------|-------|---------|--------|
| | Sport | Matic | Moped | Sport | Matic | Moped | CO | Power | CO | Power | CO | Power |
| 1 | 2.13 | 4.05 | 3.59 | 9.84 | 7.23 | 3.92 | 3.25 | 7.00 | 1.00 | 2.97 | -10.642 | 15.025 |
| 2 | 1.97 | 3.85 | 3.39 | 9.96 | 7.16 | 4.14 | 3.07 | 7.09 | 0.98 | 2.91 | -10.162 | 15.231 |
| 3 | 1.82 | 3.68 | 3.07 | 8.44 | 7.21 | 4.19 | 2.86 | 6.61 | 0.95 | 2.18 | -9.577 | 15.181 |
| 4 | 2.16 | 4.09 | 3.63 | 6.91 | 6.57 | 3.78 | 3.29 | 5.75 | 1.01 | 1.72 | -10.737 | 14.169 |
| 5 | 1.97 | 3.89 | 3.41 | 9.84 | 7.19 | 3.78 | 3.09 | 6.94 | 1.00 | 3.04 | -10.236 | 14.849 |
| 6 | 2.20 | 4.26 | 4.33 | 10.04 | 6.86 | 4.33 | 3.59 | 7.08 | 1.21 | 2.86 | -11.581 | 15.267 |
| 7 | 1.90 | 3.75 | 3.12 | 9.93 | 7.17 | 4.16 | 2.92 | 7.09 | 0.94 | 2.89 | -9.746 | 15.253 |
| 8 | 1.79 | 3.62 | 3.06 | 10.00 | 7.19 | 4.15 | 2.82 | 7.12 | 0.94 | 2.92 | -9.465 | 15.265 |
| 9 | 1.95 | 3.79 | 3.33 | 9.94 | 7.21 | 3.61 | 3.02 | 6.92 | 0.96 | 3.17 | -10.025 | 14.682 |
| 10 | 1.76 | 3.58 | 3.01 | 9.92 | 7.17 | 4.13 | 2.78 | 7.07 | 0.93 | 2.90 | -9.354 | 15.223 |
| 11 | 2.21 | 4.30 | 3.72 | 9.94 | 7.16 | 4.20 | 3.41 | 7.10 | 1.08 | 2.87 | -11.077 | 15.291 |
| 12 | 2.11 | 4.01 | 3.55 | 9.81 | 7.16 | 4.16 | 3.22 | 7.04 | 0.99 | 2.82 | -10.560 | 15.244 |
| 13 | 1.92 | 3.75 | 3.19 | 8.38 | 7.16 | 4.29 | 2.95 | 6.61 | 0.94 | 2.10 | -9.822 | 15.249 |
| 14 | 2.18 | 4.18 | 3.65 | 9.90 | 7.16 | 4.15 | 3.34 | 7.07 | 1.04 | 2.88 | -10.871 | 15.234 |
| 15 | 2.26 | 4.32 | 3.77 | 9.84 | 7.14 | 4.06 | 3.45 | 7.01 | 1.07 | 2.89 | -11.158 | 15.126 |
| 16 | 1.76 | 3.46 | 2.99 | 10.09 | 7.11 | 4.17 | 2.74 | 7.13 | 0.88 | 2.96 | -9.172 | 15.247 |
| 17 | 1.87 | 3.73 | 3.10 | 9.97 | 6.94 | 4.12 | 2.90 | 7.01 | 0.95 | 2.93 | -9.685 | 15.083 |
| 18 | 2.03 | 3.95 | 3.52 | 10.34 | 7.19 | 4.71 | 3.17 | 7.42 | 1.01 | 2.82 | -10.430 | 15.836 |

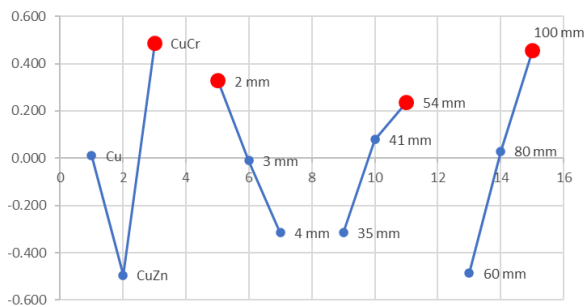


Figure 3. Effect plot S/N ratio of CO emission

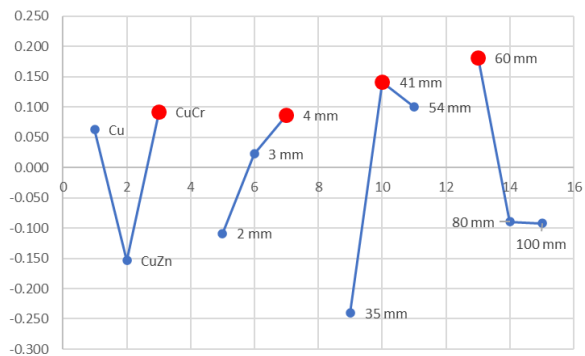


Figure 4. Effect plot S/N ratio of power

3.3. MCC Optimum Parameter Prediction

Referring to the effect plot that has been produced, it can be seen that the combination of each MCC parameter used has a positive effect on reducing CO emissions based on the prediction results. The prediction of the optimal MCC design combination that is able to optimally reduce CO emissions is presented in Table 5.

Table 5 shows the results of the predicted optimum design for CO emission, so that to determine the accuracy of the predictions, verification is required through experimental testing in the laboratory. In addition, it is necessary to predict the value of the S/N ratio using the additive predictive model before

conducting the experimental test. It aims to measure how accurate the value of the S/N ratio is from the resulting CO emission. The magnitude of the value of the S/N ratio of CO emission through the approximation method can be done using Equation (3). In addition, the value of the S/N ratio of power resulting from the combination shown in Table 4, can also be measured using this equation.

$$S/N_{pre} = \mu + Mtl_{mn} + Ch_{mn} + Cd_{mn} + Cl_{mn} \quad (3)$$

Where, S/N_{pre} = optimum S/N ratio prediction; μ = system average; Mtl_{mn} = main effect material (Mtl) at level n; Ch_{mn} = main effect curve height (Ch) at level n; Cd_{mn} = main effect cylinder diameter (Cd) at level n; and Cl_{mn} = main effect Panjang silinder (Cl) at level n.

Based on the data from Table 4, the predicted value of the S/N ratio of CO emission can be calculated using Eq. (4) and Eq. (5).

Table 6 shows the predicted results of the optimum power design that is generated from the prediction side. To know the accuracy of the predictions, it is necessary to verify them through experimental testing in the laboratory. In addition, the prediction of the value of the S/N ratio also needs to be used before conducting experimental tests. It aims to measure how accurate the value of the S/N ratio of the generated power is. The value of the S/N ratio of the power through the approach method can be determined by using Equation 3. In addition, the value of the S/N ratio of the resulting CO emission can also be used as the equation. Furthermore, the process of calculating the predicted value of the S/N ratio can be shown as follows Eq. (6) and Eq. (7).

$$\begin{aligned} S/N_{pre_3133_CO} &= \mu + Mtl_{m3} + Ch_{m1} + Cd_{m3} + Cl_{m3} \\ &= -10.239 + 0.485 + 0.327 + 0.235 + 0.456 \\ &= -8.736 \end{aligned} \quad (4)$$

$$\begin{aligned} S/N_{pre_3133_power} &= \mu + Mtl_{m3} + Tl_{m1} + Ds_{m3} + Ps_{m3} \\ &= 15.137 + 0.091 + (-0.109) + 0.100 + (-0.092) \\ &= 15.127 \end{aligned} \quad (5)$$

$$\begin{aligned} S/N_{pre_3321_power} &= \mu + Mtl_{m3} + Ch_{m1} + Cd_{m3} + Cl_{m3} \\ &= 15.137 + 0.091 + 0.086 + 0.141 + 0.181 \\ &= 15.636 \end{aligned} \quad (6)$$

$$\begin{aligned}
 S/N_{pre_3321_CO} &= \mu + Mtl_{m3} + Ch_{m1} + Cd_{m3} + Cl_{m3} \\
 &= -10.239 + 0.485 + (-0.316) + 0.080 + (-0.486) \\
 &= -10.476
 \end{aligned}
 \tag{7}$$

Table 5. Optimum design prediction of CO emission

| CO Emission | Materials | Curve height | Cylinder diameter | Cylinder length |
|----------------|-----------|--------------|-------------------|-----------------|
| Optimum Design | Level 3 | Level 1 | Level 3 | Level 3 |
| | CuCr | 2 mm | 54 mm | 100 mm |

Table 6. Optimum design prediction of power

| Power Optimum | Materials | Curve height | Cylinder diameter | Cylinder length |
|---------------|-----------|--------------|-------------------|-----------------|
| Design | Level 3 | Level 3 | Level 2 | Level 1 |
| | CuCr | 4 mm | 41 mm | 60 mm |

3.4. Result Verification

After the calculation of the optimum design predictions for CO and power had been carried out, the next step was to verify through experimental tests in the laboratory. Furthermore, the experimental test results for the optimum CO design are presented in [Table 7](#).

Based on the experimental test results, it is found that the optimum design of CO emission produced through the optimization process has a better S/N value of CO emission ratio when compared to 18 designs from L18. Therefore, it can be stated that the optimal design of CO emission obtained based on the robust parameter design method is proven to be accurate according to the predictions. If further analysis is carried out, by comparing the predicted results with the experimental test results, the results can be seen in the following [Table 8](#).

Referring to [Table 8](#), it is observed that the S/N value of the CO emission ratio produced through the experimental test of -8.973 has a better tendency than the predicted S/N ratio value of -8.736. However, the predicted results are considerably acceptable because the error rate generated is only 2.6%. Furthermore, from the

optimum design of this CO, it also produces a precise power value. This is because the resulting error rate between the predicted and experimental results is only 0.9%, where the S/N ratio of the predicted power is 15.127 while the S/N ratio of the power of the experimental test results is 15.269. This finding is in line with research Abas et al. [31] which revealed that the S/N ratio is an effective technique for optimizing the performance of an experimental design. Furthermore, design verification was also carried out on the optimum power design, where the experimental test results are presented in the [Table 9](#).

Based on the experimental test results, it is known that the optimum power design produced is accommodated in 18 designs from L18, the optimum power design is shown through experimental results 18. Therefore, it can be stated that the optimal power design obtained based on the robust parameter design method is proven to be accurate according to the predictions. If further analysis is carried out, by comparing the predicted results with the experimental test results, the results can be seen in the following [Table 10](#).

Table 7. CO optimum design prediction verification results

| Mtl | Ch | Cd | Cl | Mean | | STDEV | | S/N Ratio | |
|-------|-------|-------|--------|------|-------|-------|-------|-----------|--------|
| | | | | CO | Power | CO | Power | CO | Power |
| lvl 3 | lvl 1 | lvl 3 | lvl 3 | 2.66 | 7.11 | 0.89 | 2.92 | -8.973 | 15.269 |
| CuCr | 2 mm | 54 mm | 100 mm | | | | | | |

Table 8. Comparison between predicted results and experimental tests for optimum CO

| Output | | Prediction | Experimental | Error |
|-----------|-------|------------|--------------|-------|
| S/N Ratio | CO | -8.736 | -8.973 | 2.6% |
| | Power | 15.127 | 15.269 | 0.9% |

Table 9. Optimum power design prediction verification results

| Mtl | Ch | Cd | Cl | Mean | | STDEV | | S/N Ratio | |
|---------------|---------------|----------------|----------------|------|-------|-------|-------|-----------|--------|
| | | | | CO | Power | CO | Power | CO | Power |
| Lvl 3 CuCr | Lvl 3 4 mm | Lvl 2 41 mm | Lvl 1 60 mm | 3.17 | 7.42 | 1.01 | 2.82 | -10.430 | 15.836 |

Table 10. Comparison between predicted results and experimental tests of optimum power

| Output | Prediction | Experimental | Error | |
|-----------|------------|--------------|---------|-------|
| S/N Ratio | CO | -10.430 | -10.476 | 0.4% |
| | Power | 15.836 | 15.636 | -1.3% |

Referring to [Table 10](#), it is seen that the S/N power ratio value generated through the experimental test of 15,836 has a better tendency than the predicted S/N ratio value of 15,636. The prediction results are considered accurate because the error rate generated is only 0.4%. Furthermore, the optimum power design also produces a fairly accurate CO emission value. This is because the resulting error rate between the predicted and experimental results is only -1.3%, where the S/N ratio of the predicted power is -10,430 while the S/N ratio of the power of the experimental test results is -10,476. These findings support the theory that the S/N ratio approach can provide reliable estimates to understand the impact of controlled parameters on experimental results [32].

Overall, these two MCC designs demonstrate optimal performance in different aspects. The CO optimum design shows very good performance in reducing CO emissions with high power precision. In contrast, the power optimum design shows a significant increase in power with adequate accuracy in CO emission reduction. It is important to note that the primary focus in the development of these MCC designs is to reduce CO emissions, while also considering power. In this case, the CO optimum design is the best choice as it provides more significant and accurate CO emission reduction and results that are closer to predicted values with a higher accuracy percentage. This indicates the potential of MCCs to offer efficient and effective solutions for reducing vehicle emissions.

3.5. Improved CO Emission and Power Optimization Results

After obtaining the results of the optimum CO design, the next step is to compare the results between the MCC standard of Platinum Group Metal (STD PGM) and the optimum CO design.

STD PGM exhaust is a type of exhaust generally produced by the motorcycle industry and uses Platinum Group Metal (PGM) such as platinum, palladium, and rhodium as catalyst materials. The basic design of a standard PGM exhaust includes its physical construction and catalyst material composition as defined by industry standards. The results of the comparison of optimum CO design and STD PGM can be seen in [Table 11](#).

Based on [Table 11](#) it is seen that the gain is the difference between optimum CO and STD PGM. From these results, the optimum CO does not perform as well as STD PGM in terms of its ability to reduce exhaust emissions. This is normal because STD PGM uses materials derived from precious metals. Khivantsev et al. [33] explained that catalysts derived from precious metals can reduce CO emissions by up to 99%, while HC emissions can be reduced by up to 95%.

However, when viewed from the difference, which is only -0.372 adrift of course, the E19 can be an alternative. Another advantage of this design is that it is relatively cheaper with the availability of abundant materials. In terms of CO emission, STD PGM tends to be better than the optimum CO design. However, when viewed from the power value generated, the optimum CO design is superior by a difference of 5,037 compared to the STD PGM. In more detail, the comparison between the core and the optimum CO design can be done through the experimental test results.

Meanwhile, from the optimum power or experimental design 18 (E18), the next step was to compare the results between the standard MCC of precious metals (STD PGM), hereinafter referred to as STD PGM, and optimum power design, hereinafter referred to as optimum power. The results of the comparison of optimum power design and STD PGM are shown in [Table 12](#).

Table 11. Comparison of STD PGM and Optimum CO

| | STD PGM | Optimum CO | Gain |
|-----------------|---------|------------|--------|
| S/N Ratio CO | -8.601 | -8.973 | -0.372 |
| S/N Ratio Power | 10.232 | 15.269 | 5.037 |

Table 12. Comparison of STD PGM and E18 optimum power

| | STD PGM | E19 | Gain |
|-----------------|---------|---------|--------|
| S/N Ratio CO | 10.232 | 15.636 | 5.404 |
| S/N Ratio Power | -8.601 | -10.476 | -1.875 |

Based on [Table 12](#), it is seen that the optimum power design can surpass STD PGM in terms of the ability to increase vehicle power. This is normal because the design of the inlet and outlet angles on the optimum power design is made in such a way that it forms an angle of 10° for in and 15° for out angle. Bell [32] through his book suggests that the exhaust gas flow in the MCC housing can run optimally if modifications are made to the inlet taper with an angle of 10° and the outlet taper with an angle of 15°. Not only that, the ability of optimum power design to reduce CO emissions also needs to be taken into account. This is because the STD PGM excels only by a difference of -1,875, meaning this design is also worthy of consideration as an alternative MCC to replace the STD PGM.

4. Conclusion

Based on the results of testing and research discussions that have been carried out, the following conclusions are drawn.

1. The best MCC design that can reduce CO emissions is the STD PGM. However, the optimum CO design can be used as an alternative because the difference in the S/N ratio is only -0.372. Meanwhile, the optimum CO design has another advantage over the STD PGM, namely the value of the S/N power ratio which tends to be higher with a difference of 5,037 compared to the STD PGM.
2. The best MCC design that can increase power is the optimum power design. The optimum power design has a superior S/N ratio with a difference of 5,404. In terms of emission, the E18 tends to be lower by a difference of -1,875 compared to the STD PGM.

Acknowledgements

Many thanks to the Engine Performance Testing Laboratory, Department of Mechanical

Engineering, Faculty of Engineering, Universitas Negeri Surabaya which has provided facilities for the researcher to collect data.

Author's Declaration

Authors' contributions and responsibilities

The authors made substantial contributions to the conception and design of the study. The authors took responsibility for data analysis, interpretation and discussion of results. The authors read and approved the final manuscript.

Funding

There is no funding information from authors.

Availability of data and materials

All data are available from the authors.

Competing interests

The authors declare no competing interest.

Additional information

No additional information from the authors.

References

- [1] United Nations, "The Sustainable Development Goals Report 2017," New York, 2017.
- [2] UNDP, *Sustainable Development Goals*. United Nations Development Programme (UNDP).
- [3] A. Sule, Z. A. Latiff, M. A. Abbas, I. Veza, and A. C. Opia, "Recent Advances in Diesel-Biodiesel Blended with Nano-Additive as Fuel in Diesel Engines: A Detailed Review," *Automotive Experiences*, vol. 5, no. 2, pp. 182–216, 2022, doi: 10.31603/ae.6352.
- [4] B. O. Bolaji, D. O. Bolaji, and S. T. Amosun, "Energy and cooling performance of carbon-dioxide and hydrofluoroolefins blends as eco-friendly substitutes for R410A in air-conditioning systems," *Mechanical Engineering for Society and Industry*, vol. 3, no. 1, pp. 35–46, 2023, doi: 10.31603/mesi.8591.
- [5] M. Masoudi, J. Hensel, and E. Tegeler, "A

- Review of the 2018 U.S.-DOE CLEERS Conference: Trends and Deeper Insights in Reduction of NO_x and Particulate in Diesel and Gasoline Engines and Advances in Catalyst Materials, Mechanisms, and Emission Control Technologies," *Emission Control Science and Technology*, vol. 6, no. 2, pp. 113–125, Jun. 2020, doi: 10.1007/s40825-019-00134-1.
- [6] H. Dong, J. Zhao, J. Chen, Y. Wu, and B. Li, "Recovery of platinum group metals from spent catalysts: A review," *International Journal of Mineral Processing*, vol. 145, pp. 108–113, Dec. 2015, doi: 10.1016/j.minpro.2015.06.009.
- [7] Warju, *Teknologi Reduksi Emisi Gas Buang Kendaraan Bermotor*. Surabaya: Unesa University Press, 2013.
- [8] P. Lang, N. Yuan, Q. Jiang, Y. Zhang, and J. Tang, "Recent Advances and Prospects of Metal-Based Catalysts for Oxygen Reduction Reaction," *Energy Technology*, vol. 8, no. 3, p. 1900984, Mar. 2020, doi: 10.1002/ente.201900984.
- [9] P. Choudhury and S. Deo, "An Innovative Approach for Emission Control Using Copper Plate Catalytic Converter," *International Journal of Advanced Science, Engineering and Technology*, vol. 3, no. 2, pp. 19–23, 2014.
- [10] S. Rathore, M. Thakur, and S. S. . Deepak, "Modeling and Simulation of Four Stroke Spark Ignition Engine with Nano-Particle Coated Catalytic Converter for Analysis of Exhaust Emissions," *International Journal for Research in Applied Science and Engineering Technology*, vol. 6, no. 6, pp. 1447–1456, 2018, doi: 10.22214/ijraset.2018.6212.
- [11] I. A. N. N. Shoffan, S. Sumarli, and I. M. Nauri, "The effect of copper-based catalytic converter with circular tube shape on exhaust emission of Yamaha Vixion 1PA," *IOP Conference Series: Materials Science and Engineering*, vol. 669, no. 1, pp. 0–9, Nov. 2019, doi: 10.1088/1757-899X/669/1/012014.
- [12] Sukarman *et al.*, "Optimization of tensile-shear strength in the dissimilar joint of Zn-coated steel and low carbon steel," *Automotive Experiences*, vol. 3, no. 3, pp. 115–125, 2020, doi: 10.31603/ae.v3i3.4053.
- [13] A. D. Shieddieque, Sukarman, Mardiyati, B. Widyanto, and Y. Aminanda, "Multi-objective Optimization of Sansevieria Trifasciata FibreReinforced Vinyl Ester (STF/VE) Bio-composites for the Sustainable Automotive Industry," *Automotive Experiences*, vol. 5, no. 3, pp. 288–303, 2022, doi: 10.31603/ae.7002.
- [14] S. R. Ariyanto, S. Suprayitno, and R. Wulandari, "Design of Metallic Catalytic Converter using Pareto Optimization to Improve Engine Performance and Exhaust Emissions," *Automotive Experiences*, vol. 6, no. 1, pp. 200–215, Apr. 2023, doi: 10.31603/ae.7977.
- [15] R. Nawaz, I. Hussain, S. Noor, T. Habib, and M. Omair, "The significant impact of the economic sustainability on the cement industry by the assessment of the key performance indicators using Taguchi signal to noise ratio," *Cogent Engineering*, vol. 7, no. 1, p. 1810383, Jan. 2020, doi: 10.1080/23311916.2020.1810383.
- [16] L.-H. Ho, S.-Y. Feng, and T.-M. Yen, "A New Methodology for Customer Satisfaction Analysis: Taguchi's Signal-to-Noise Ratio Approach," *Journal of Service Science and Management*, vol. 07, no. 03, pp. 235–244, 2014, doi: 10.4236/jssm.2014.73021.
- [17] J. Liu *et al.*, "Dynamic Evaluation Method of Machining Process Planning Based on Digital Twin," *IEEE Access*, vol. 7, pp. 19312–19323, 2019, doi: 10.1109/ACCESS.2019.2893309.
- [18] SNI 19-7118.3-2005, *Emission of Moving-Source-Moving Gas-Part 3: Test Methods for Category L Motor Vehicles at Idle Conditions*. 2005.
- [19] SAE J1349, *Engine Power Test Code-Spark Ignition and Compression Ignition-Net Power Rating*. Warrendale: SAE International, 2004.
- [20] P. U. Arvikar, "The Performance of Modified Catalytic Converter using Copper-Nickel as Catalysts to Reduce Exhaust Gas Emissions from CI Engine," *International Journal for Research in Applied Science and Engineering Technology*, vol. 7, no. 6, pp. 1536–1542, Jun. 2019, doi: 10.22214/ijraset.2019.6260.
- [21] Warju, S. P. Harto, and Soenarto, "The Performance of Chrome-Coated Copper as Metallic Catalytic Converter to Reduce

- Exhaust Gas Emissions from Spark-Ignition Engine," *IOP Conference Series: Materials Science and Engineering*, vol. 288, no. 1, p. 012151, Jan. 2018, doi: 10.1088/1757-899X/288/1/012151.
- [22] A. C. Mitra, M. Jawarkar, T. Soni, and G. R. Kiranchand, "Implementation of Taguchi Method for Robust Suspension Design," *Procedia Engineering*, vol. 144, pp. 77–84, 2016, doi: 10.1016/j.proeng.2016.05.009.
- [23] A. Rout, S. S. Sahoo, S. Singh, S. Pattnaik, A. K. Barik, and M. M. Awad, "Benefit-cost analysis and parametric optimization using Taguchi method for a solar water heater," in *Design and Performance Optimization of Renewable Energy Systems*, Elsevier, 2021, pp. 101–116.
- [24] E. Ginting and M. M. Tambunan, "Selection of Optimal Factor Level From Process Parameters in Palm Oil Industry," *IOP Conference Series: Materials Science and Engineering*, vol. 288, p. 012056, Jan. 2018, doi: 10.1088/1757-899X/288/1/012056.
- [25] S. Yu, G. Dai, Z. Wang, L. Li, X. Wei, and Y. Xie, "A consistency evaluation of signal-to-noise ratio in the quality assessment of human brain magnetic resonance images," *BMC Medical Imaging*, vol. 18, no. 1, p. 17, Dec. 2018, doi: 10.1186/s12880-018-0256-6.
- [26] M. Ramachandran and N. Agarwal, "Identification of Most Affected Parameter for Design for Remanufacturing of Scrap Piston by Taguchi Desirability Function Analysis," 2018, pp. 320–329.
- [27] M. Ilevbare and O. M. Omorogieva, "Formation evaluation of the petrophysical properties of wells in e - field onshore Niger Delta, Nigeria," *Nigerian Journal of Technology*, vol. 39, no. 4, pp. 962–971, Mar. 2021, doi: 10.4314/njt.v39i4.1.
- [28] R. K. Verma, D. Patel, and M. K. Chopkar, "Wear behavior investigation of Al-B4C functionally graded composite through Taguchi's design of experiment," *Journal of Engineering Research*, p. 100095, May 2023, doi: 10.1016/j.jer.2023.100095.
- [29] O. S. Ogbonna, S. A. Akinlabi, N. Madushele, O. S. Fatoba, and E. T. Akinlabi, "Grey-based taguchi method for multi-weld quality optimization of gas metal arc dissimilar joining of mild steel and 316 stainless steel," *Results in Engineering*, vol. 17, p. 100963, Mar. 2023, doi: 10.1016/j.rineng.2023.100963.
- [30] J. Antony, "Case Studies," in *Design of Experiments for Engineers and Scientists*, Elsevier, 2014, pp. 125–188.
- [31] M. Abas *et al.*, "Experimental Investigation and Statistical Evaluation of Optimized Cutting Process Parameters and Cutting Conditions to Minimize Cutting Forces and Shape Deviations in Al6026-T9," *Materials*, vol. 13, no. 19, p. 4327, Sep. 2020, doi: 10.3390/ma13194327.
- [32] N. Mansour, M. Marschall, T. May, A. Westermann, and T. Dau, "A method for realistic, conversational signal-to-noise ratio estimation," *The Journal of the Acoustical Society of America*, vol. 149, no. 3, pp. 1559–1566, Mar. 2021, doi: 10.1121/10.0003626.
- [33] K. Khivantsev *et al.*, "Palladium/Zeolite Low Temperature Passive NO_x Adsorbers (PNA): Structure-Adsorption Property Relationships for Hydrothermally Aged PNA Materials," *Emission Control Science and Technology*, vol. 6, no. 2, pp. 126–138, Jun. 2020, doi: 10.1007/s40825-019-00139-w.